Iraqi Journal of Science, 2020, Vol. 61, No.1, pp: 1-12
DOI: 10.24996/ijs.2020.61.1.1

ISSN: 0067-2904

Electro polymerization for (N-Terminal tetrahydrophthalamic acid) for Anti-corrosion and Biological Activity Applications

Khulood A.Saleh, Mayasa I.Ali*
Department of Chemistry, College of Science, University of Baghdad, Baghdad, Iraq

Received: 23/6/ 2019 Accepted: 18/ 8/2019

Abstract
The present work reports the electrochemical synthesis of poly N Terminal tetrahydrophthalamic acid on stainless steel 316 (S.S), which acts as a working electrode, using an electrochemical polymerization technique. Fourier Transform Infrared Spectroscopy (FT-IR), Atomic Force Microscope (AFM) and Scanning Electron Microscope (SEM) characterized the formed polymer film. Corrosion protection tests for coated and uncoated S.S with polymer film were studied in 0.2 M hydrochloric acid (HCl) solution by using electrochemical polarization technique. Kinetic and thermodynamic activation parameters (Ea, A, ΔH*, ΔS* and ΔG*) were calculated. The biological activity of the polymeric film was determined against Gram positive (*Staphylococcus aureus*; *Staph.aure*) and negative bacteria (*Escherichia coli*; *E.coli*).In addition, the polymer film was modified with nanomaterials(ZnO_nnano and Graphene).

Keywords: Nanomaterial, Corrosion, Electrochemical polymerization, Conductivepolymers, Biological activity

البلمرة الكهربائية ل (N-تيرامينويل رباعي الهيدروجين حامض الفثاليك) لتطبيقات مضادات التآكل والفعالية البيولوجية

خلود عبد صالح، مياسة عصام علي*
قسم الكيمياء، كلية العلوم، جامعة بغداد، بغداد، العراق

الخلاصة
يتضمن هذا البحث تحضير طبقة بولي (N-تيرامينويل رباعي الهيدروجين حامض الفثاليك على سطح الفولاذ المقاوم نوع 316 والذي يمثل القطب العامل بأستخدام تقنية البلمرة الكهربائية. وقد شخصت البوليمر المحضر باستخدام مطياف الاشعة تحت الحمراء, مجهر القوة الذرية و مجهر المسح الالكتروني. تم دراسة قياسات التآكل للعينات الغير مطلية والمطلية بالطبقة البوليمرية في محلول حامض الهيدروكلوريك المخفف بتركيز 0.2 مولاري وفي المدى الحراري (293-323)كلفن. وايضا تم حساب الدوال الحركية والثرموديناميكية لحالة الانتقال لعملية التآكل. تضمن البحث دراسة الفعالية البيولوجية للبوليمر المحضر ضد سلالات البكتريا وهي المكورات العنقودية الذهبية و الاشريكية القولونية. وتم استخدام المواد النانوية (اوكسيد الزنك النانويوالكرافين) لزيادة كفاءة الطبقة البوليمرية ضد التآكل والبكتريا.

1. Introduction
Corrosion is basically an economic problem. Therefore, the corrosion behavior of materials is an important consideration in the economic evaluation of any project. It is not always wise to select the

*Email:chemistmayasa@gmail.com

material with the lowest initial costsince it is not necessarily the ultimate cost. Overall costs involve downtime, maintenance, tax aspects, time value of money and obsolescence [1]. Corrosion is the interaction of a material with its environment [2]. One of the methods that was used for corrosion protection is the conductive polymers coating, with the synthesis of conducting polymers can be carried out by using electrochemical polymerization techniques[3]. Electrochemical polymerization occurs when a suitable anodic potential or current is applied to a conducting substrate that has been immersed in a monomer electrolyte.The formation of a dense and homogenous distribution of chemical bonds between the substrate and the polymer would resist chemical attack and mechanical stress from the environment. A wide range of electrochemical techniques can be used for electrochemical polymerization, but galvanostatic (constant current), potentiostatic (constant potential) and potential sweeping techniques, such as cyclic voltammetry, are the methods that are generally employed [4]. Conducting polymers have attracted a great attention due to their excellent properties in different technological applications such as chemical sensors (e.g.biosensor) [5- 7], molecular electronic devices (e.g. diodes and field effect transistors) [8], batteries [9], biomedical engineering [10], corrosion inhibitors [11-13],electrochromic devices[14, 15], supercapacitors [16,17], electroluminescence [18], photovoltaic cells [19, 20],dye sensitized solar cells (DSSCs) [21], and biofuel cells [22]. The use of coating which has antimicrobial activity is an effective method for decreasing microbial numbers on healthcare surfaces. Antimicrobial agents are materials that have the ability for killing pathogenic microorganism [23].Good antimicrobial polymers should be biocidal to abroad spectrum of pathogenic microorganism, can be regenerated upon loss of activity, insoluble in water for variable applications, and cannot be decomposed to toxic materials [24]. In this paper, an electrochemical polarization technique was applied to study the protection efficiency of the conductive polymer film on the corrosion of S.S in 0.2 M of HCl solution at a temperature range of293-323K. The effect of adding nanomaterials (Graphene and ZnO(nano)) on the anticorrosion action of the polymer film on S.S surfaces is investigated.

2.Experimental part

The electrochemical polymerization of N-Termenoiyl tetrahydrephthalamic acid (monomer) onto the S.S surface was carried out in a monomer solution using a DC power supply and two electrodes, namely the working electrode (WE) and the country electrode (CE) (Galvanostatic technique), as shown in Figure-1. The electrodes were polished by different grades of silicon carbide (800, 1200 and 2000 mesh grit), then washed by D.W. and acetone and kept in a desiccator. The solution employed for electrochemical polymerization consisted of 0.1 g of N- Termenoiyl tetrahydrophthalamic acid in 100 mlH_2O with three drops of H_2SO_4(95%) [25]. For corrosion measurements, S.S was used as a WE , \platinum as an axillary electrode, and saturated calomel electrode (SCE) as a reference electrode. Cathodic and anodic polarization of S.S was carried out under potentiostatic conditions in 0.2 M HCl solution and at a temperature range of 293-323K. In addition,0.04gof ZnO (nano) and 0.004g of graphene were added to increase the efficiency of polymer film against corrosion. Equation 1shows the electrochemical polymerization for the monomer.

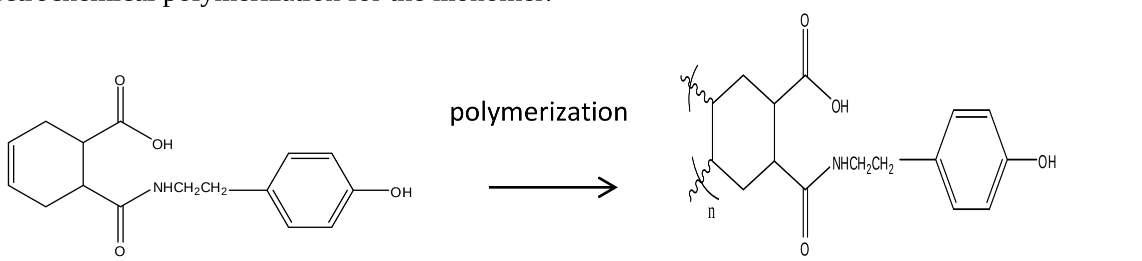

N-Terminaltetrahydrophthalamic acid

Poly (N-Terminaltetrahydrophthalamic acid)

Equation1- Conversion of the monomer into a polymer.

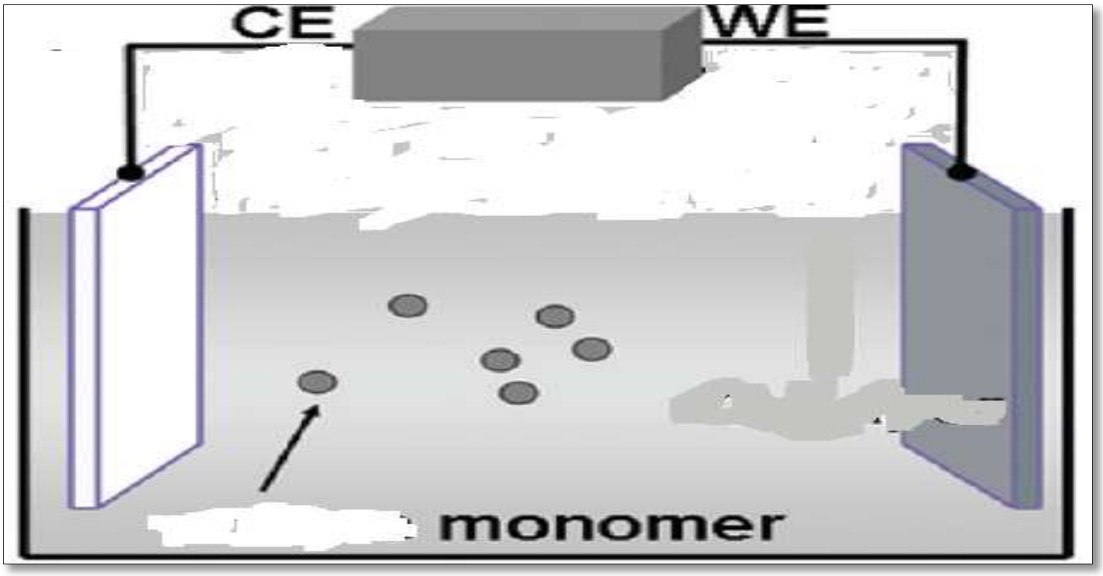

Figure 1-Electrochemical polymerization technique

3.Results and Discussion

3.1. Mechanism of polymerization

The cationic mechanism [26, 27] explains the electrochemical polymerization process, as in the following steps.

-Cationic mechanism (Scheme1): the application of the anodic potential to the monomers solutions implied the following:

A1: one electron is transferred from the monomer to the electrode.

A2: the transfer of the electron in A1 led to the formation of a radical cation which is adsorbed on the surface of the electrode.

A3: the radical cation is desorbed and reacted in the solution to increase the molecular weight of the species.

A4: the monomer molecules are added by the cationic mechanism at the charged end of the oxidized monomer.

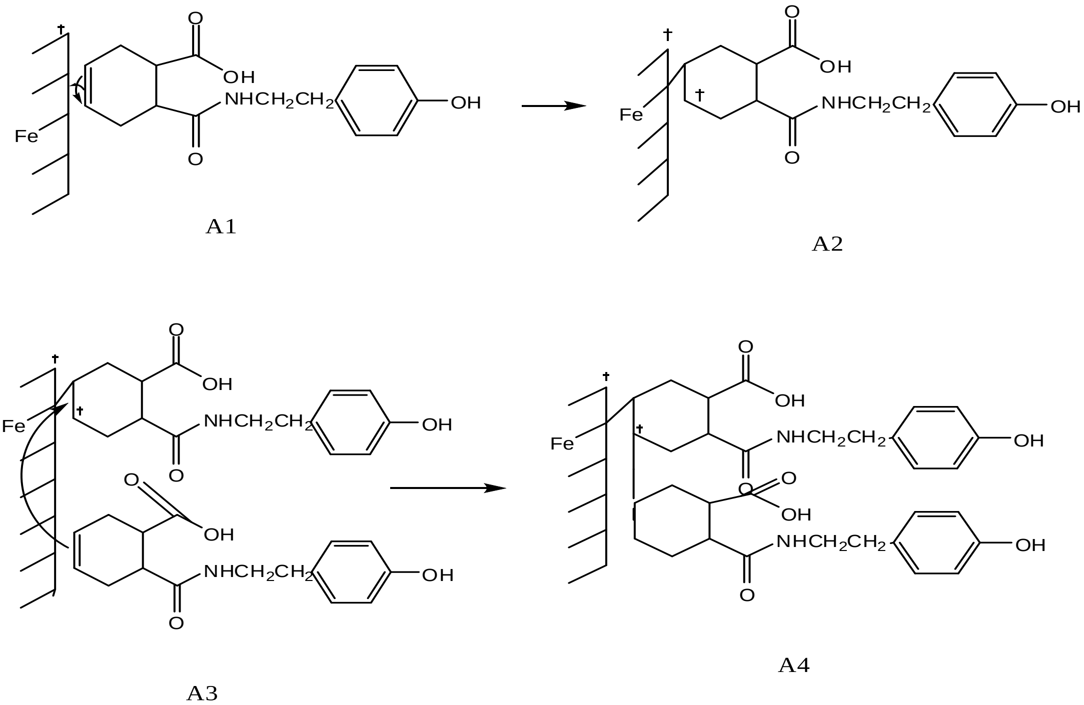

Scheme1-Cationic mechanism for polymer film on S.S.

3.2. Fourier Transmission Infrared Region(FT-IR) Spectroscopy of the synthesized polymer
The polymer film was characterized by FT-IR as shown in Figure-2b. In these spectra, the aliphatic double bond (=CH) 3128 cm^{-1}has disappeared, which confirmed the formation of the polymer.

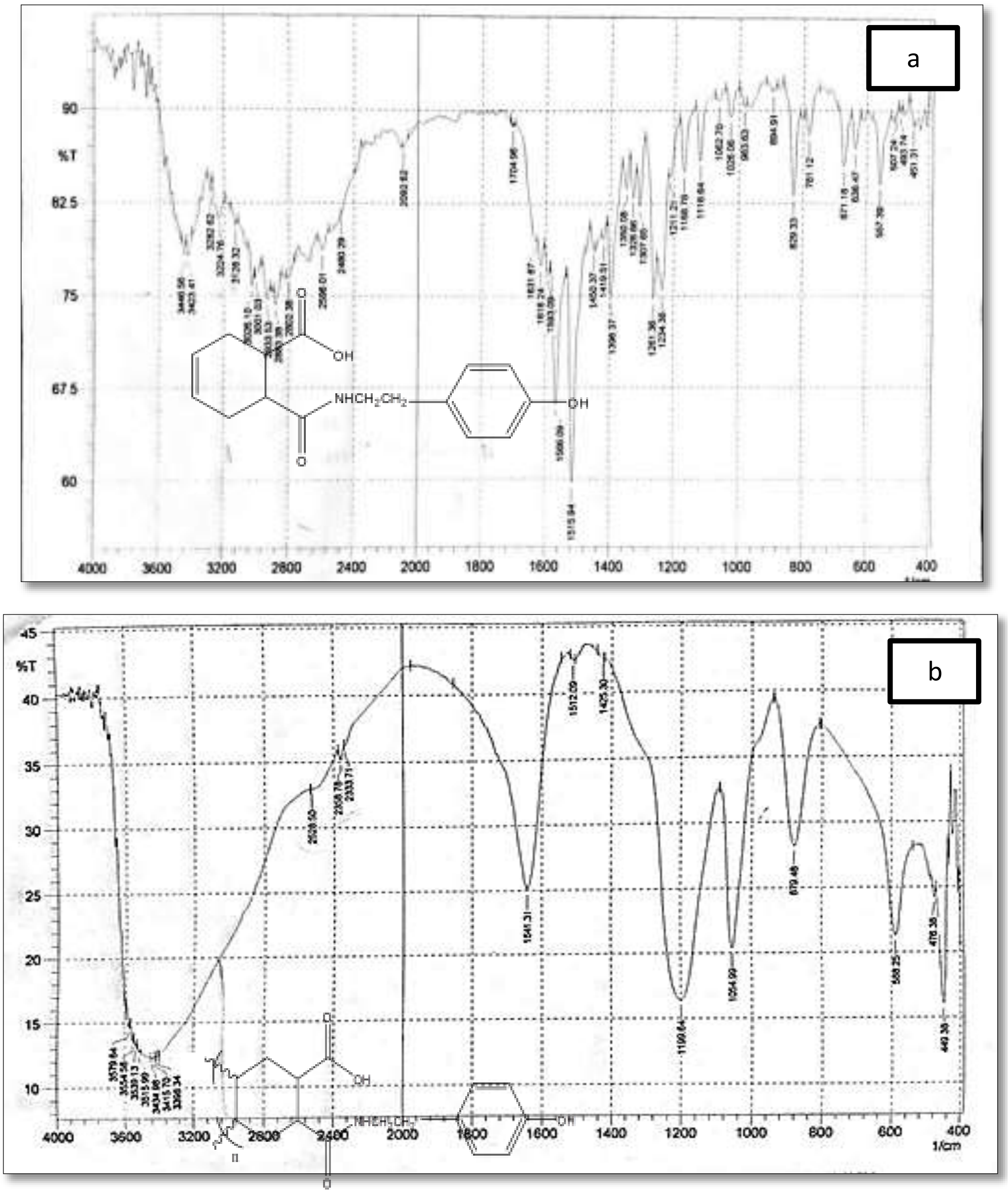

Figure 2- FT-IR for a) monomer, b) polymer.

According to Figure-1-a, the band appeared at 704.96 cm^{-1} for C=O of carboxylic acid, the band appeared at 1631.67 cm^{-1} for C=O of the amide group, the band of OH of carboxylic acid appeared at 2596.01cm^{-1}, the band of NH of amide appeared at 3224.76 cm^{-1}, the band of aromatic C=C appeared at 1593.09 cm^{-1}, the band of phenolic OH appeared at 3446.56 cm^{-1}[28-30].

3.3. Atomic Force Microscope (AFM)

AFM was employed to reveal more information, due to its function as one of the surface investigation instruments for nanoscale structure. Figure-(3a,3b,3c) shows the two and three dimensions for the prepared polymers in the absence and presence of the nanomaterial. These images show the degree of agglomeration of the nanomaterial, due to the adhesiveness of ZnO_n and G to the polymers, along with the produced smooth layers. In AFM analysis, average roughness (Ra) and Root Mean Square Roughness (RMS) are the most widely used parameters to characterize the surface roughness of the prepared polymer films. The obtained RMS and Ra values are listed in Table- 1 The results indicate a decrease in the surface roughness (increased smoothness) after modification of the polymers with the nanomaterial, due to the decrease in the grain size [31].

Table 1-Average roughness (Ra), root mean square roughness (RMS) and mean grain size for coated S.S by polymer film in the absence and presence of the nanomaterial.

system	Ra (nm)	RMS (nm)	Mean grain size (nm)
coated S.S with polymer	2.750	3.320	104.41
coated S.S with polymermodified with ZnO_n	0.992	1.190	84.72
coated S.S with polymer modified with Graphene	0.841	1.030	64.19

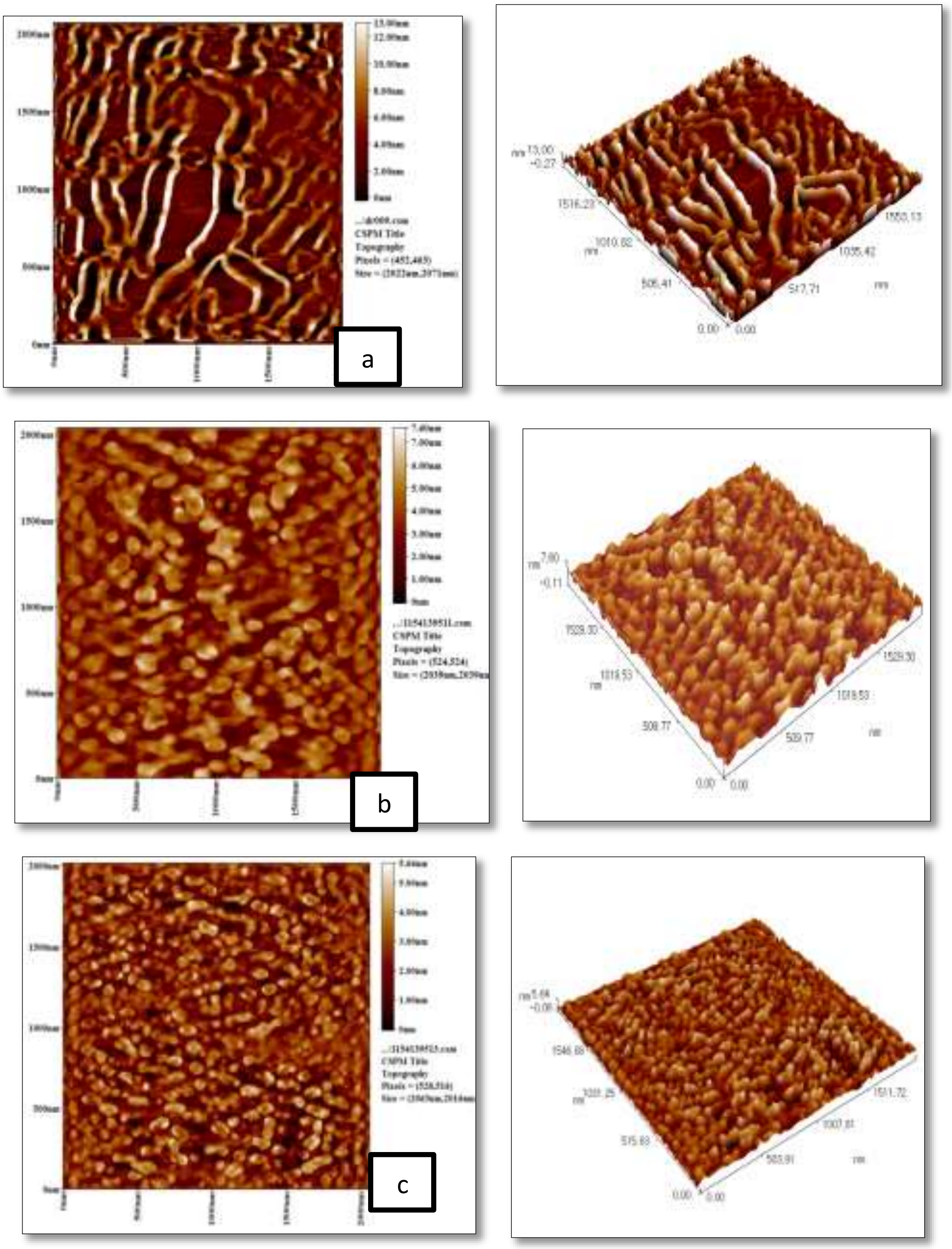

Figure3-AFM images for (a) polymer, (b) polymer modified with ZnOn, (c) polymer modified with Graphene.

3.3. Scanning Electron Microscope (SEM)

The surface morphological properties of the polymer film in the absence and presence of the nanomaterial were characterized by scanning electron microscope (SEM).Figure-4a shows that the polymer film has a non-uniform distribution on the surface of S.S. Figure-4b show the polymers film modified with ZnO_n, where ZnO_n were uniformly dispersed in the matrix. However, ZnO_n aggregations were also observed at some locations due to their hydrophilic nature and high specific surface area [32].Figure-4c shows the polymer film modified with graphene, with the strong interaction between the polymer matrix and graphenealong with the homogenous distribution of the graphene sheet in the polymer matrix[33].

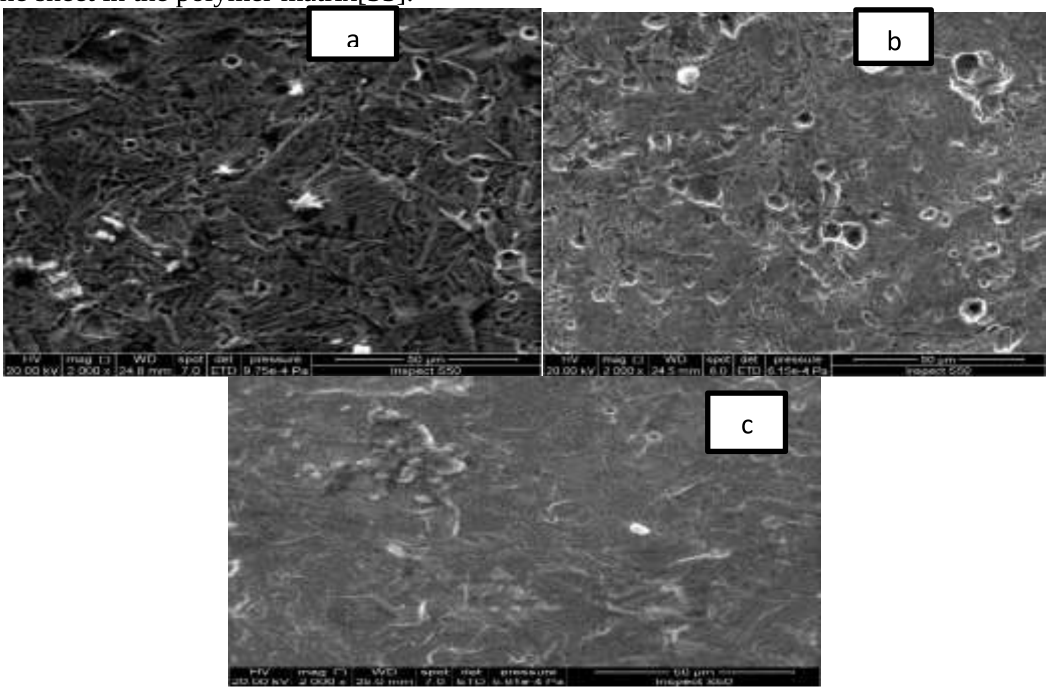

Figure 4-SEM images for a) coated S.S with polymer film, b) coated S.S with polymer film modified with ZnOn, c) coated S.S with polymer film modified with Graphene.

3.6. Potentiostate polarization curve

The corrosion parameters were evaluated from the resulting data in Table- 2 and Figure-5. The corrosion current density (icorr) and corrosion potential (Ecorr) were obtained by the extrapolation of the cathodic and anodic Tafel curves of the uncoated and coated S.S with the polymer film in HCl solution. The anodic (ba) and cathodic (bc) Tafel slopes were also calculated from Figure-5. Table-2 shows the resulting data of the corrosion potential Ecorr (mV), corrosion current density icorr ($\mu A/cm^2$), cathodic and anodic Tafel slopes bc and ba (mV/Dec), polarization resistance Rp (Ω/cm^2), weight loss WL (g/m^2.d),penetration loss PL (mm/y), and protection efficiency PE%. The data intable 2 show that the corrosion current density (icorr) and corrosion potential (Ecorr) were generally increased with temperature. Tafel plot reveals that Ecorr of the coated S.S shifts to a higher position as compared with the uncoated S.S, implying that the protection acts as an anodic protection[34]. The protection efficiency (%PE) was calculated by the following equation [35]:

$$\%\mathbf{PE} = \frac{(\mathbf{icorr})\mathbf{o} - (\mathbf{icorr})}{(\mathbf{icorr})\mathbf{o}} * \mathbf{100} \qquad \textbf{(1)}$$

Where $(i_{corr})_o$is the corrosion current density for the uncoated S.S, (i_{corr}) is the corrosion current density for the coated S.S.The polarization resistance (Rp) was determined by Stern-Gery equation [36]:

$$\mathbf{Rp} = \frac{\mathbf{ba+bc}}{\mathbf{2.303\ (ba+bc)icorr}} \qquad \textbf{(2)}$$

The polarization resistance (Rp) measurements have similar requirements to the measurements of the full polarization curves, which is auseful method to identify corrosion upsets and to initiate the remedial action. The values of Rp are listed in Table-2.

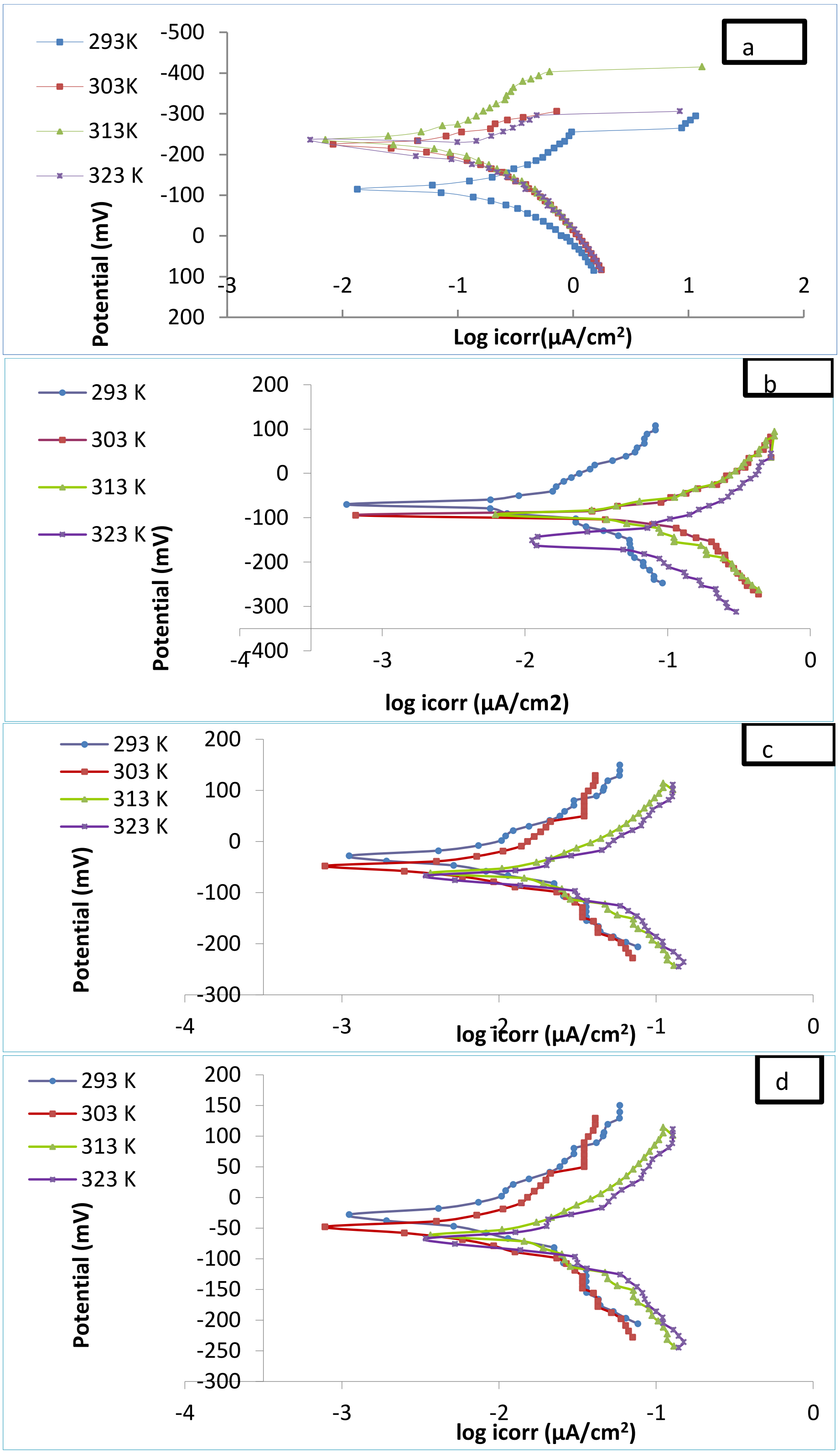

Figure 5-Polarization curves for corrosion of a) uncoated S.S, b) coated S.S with polymer film, c) coated S.S with polymer film modified with ZnOn,d) coated S.S with polymer film modified with graphene.

Table 2-Corrosion parameters for uncoated S.S and coated S.S with polymer film.

	T(K)	-Ecorr (mV)	Icorr (μA/cm²)	-bc (mV/sec)	Ba (mV/sec)	WL (g/m².d)	PL (mm/y)	PE%	Rp (Ω/cm²)
Uncoated S.S	293	113.5	43.27	48.5	47.1	3.48	0.471	-	239.786
	303	226	53.20	79.4	110.2	4.28	0.579	-	376.668
	313	235.4	56.77	149.0	120.7	4.57	0.618	-	510.035
	323	235.9	56.90	78.6	78.9	4.58	0.619	-	300.286
Coated S.S withPolymer	293	55.5	14.70	224	186.5	1.18	0.160	66.027	3006.093
	303	95.2	29.32	54.2	77.8	2.36	0.319	44.887	473.0936
	313	88.4	34.53	114.1	79.0	2.78	0.376	36.991	587.0025
	323	150.3	37.86	131.4	105.1	3.05	0.412	33.462	669.7186
Coated S.S with Polymer modified with ZnOn	293	56.2	10.06	148.2	139	0.810	0.109	76.751	3095.898
	303	71.3	15.22	135.5	182.4	1.220	0.166	71.391	2218.018
	313	223.4	19.35	205.0	245.4	1.56	0.211	65.915	2506.427
	323	187.4	19.58	201.6	266.8	1.58	0.213	65.309	2546.554
Coated S.S with Polymer modified with Graphene	293	37.5	8.00	139.6	123.7	0.644	0.087	81.511	3559.757
	303	50.0	9.88	177.5	282.6	0.795	0.108	81.429	4791.455
	313	59.8	13.11	132.4	123.5	1.06	0.143	76.907	2116.353
	323	67.1	16.32	119.8	142.0	1.31	0.177	71.318	1728.866

3.7. Kinetic and Thermodynamic Activation Parameters

Thermodynamic activation parameters involved the activation energy Ea, enthalpy of activation ΔH*, and entropy of activation ΔS*, as calculated by using the Arrhenius equation and its alternative formulation that is called the transition state.The activation energy was determined from the plot that represents the relationship between Log C.R and the reciprocal of the absolute temperature (1/T) [37], as shown in Figure-6.

$$\textbf{Log C.R} = \textbf{Log A} - \frac{\textbf{Ea}}{\textbf{2.303RT}} \qquad \textbf{(3)}$$

Where C.R: corrosion rate, A: pre-exponential factor, Ea: Activation energy, R: Gas constant (8.315 $JK^{-1}mol^{-1}$), T: Absolute temperature (K). While, the transition state is expressed in the following equation [38]:

$$\textbf{Log}\frac{\textbf{C.R}}{\textbf{T}} = \boldsymbol{Log}\left[\frac{\boldsymbol{R}}{\boldsymbol{Nh}} + \frac{\boldsymbol{\Delta S*}}{\boldsymbol{2.303R}}\right] - \frac{\boldsymbol{\Delta H*}}{\boldsymbol{2.303RT}} \qquad \textbf{(4)}$$

Where N: Avagadrous number (6.022×10^{23}mol), h: Planks constant (6.62×10^{-34} J.S). The entropy of activation ΔS* and enthalpy of activation ΔH* were determined from the plot that represents the relationship between log (C.R/T) and the reciprocal of the absolute temperature (1/T), as shown in Figure-7. Where the slope represents (- ΔH*/2.303RT) and the intercept represents (Log (R/Nh) + ΔS*/2.303R). The free energy of activation was determined from the following equation:

$$\textbf{ΔG* = ΔH* -TΔS*} \qquad \textbf{(5)}$$

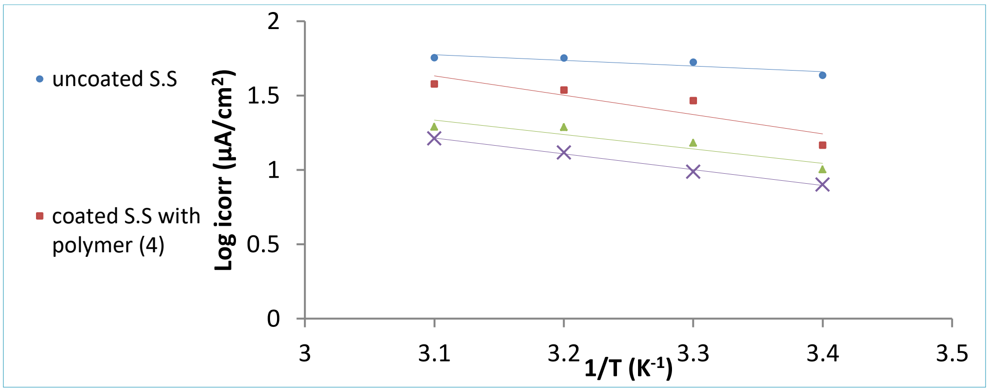

Figure 6-Plot of log icorr vs. 1/T for the uncoated & coated S.S with a polymer film in the absence and presence of the nanomaterial (ZnO_n and graphene)in 0.2M HCl solution.

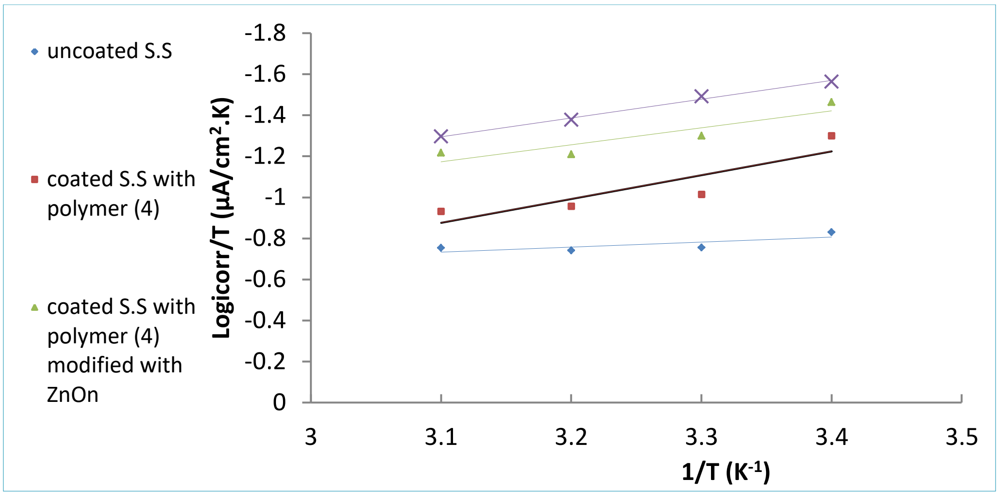

Figure 7-Plot of log icorr/T vs. 1/T for the uncoated & coated S.S with a polymer (4) in the absence and presence of the nanomaterial (ZnOn and graphene) in 0.2M HCl solution

Table 3-Transition state thermodynamic parameters at different temperatures for the corrosion of the uncoated and coated S.S with a polymer film in the absence and presence of the nanomaterial (ZnOn and graphene) in 0.2M HCl solution

coating	T(K)	ΔG* (kJ/mol)	ΔH* (kJ/mol)	-ΔS* (J/mol.K)	R^2	Ea (kJ/mol)	A (Molecule. $Cm^{-2}.S^{-1}$)	R^2
uncoated S.S	293	68.252	4.711	216.864	0.604	7.373	$5.605*10^{26}$	0.784
	303	70.421						
	313	72.589						
	323	74.758						
CoatedS.S with Polymer	293	70.468	22.233	164.624	0.783	24.9709	$2.852*10^{29}$	0.818
	303	72.114						
	313	73.760						
	323	75.407						
Coated S.S with Polymermodified with ZnOn	293	71.579	15.913	189.987	0.821	18.556	$1.317*10^{28}$	0.859
	303	73.479						
	313	75.379						
	323	77.279						
Coated S.S with Polymer modified with Graphene	293	72.417	17.579	187.162	0.993	20.279	$1.893*10^{23}$	0.994
	303	74.289						
	313	76.161						
	323	78.032						

In general, the results show that the thermodynamic activation parameters (Ea and ΔH*) for the S.S coated by the polymer film are higher than those for the uncoated S.S . This indicates an increase in the energy barrier. The values of the entropy of activation for the polymer film-coated and uncoated S.S are negative, indicating that the activated complex in the rate-determining step was achieved in an association rather than a dissociation step, along with a decreased disordering which occurs upon moving from reactants to activated complex [39]. The free energy activation had positive values, as shown in Table- 3.In addition, almost a small change is shown with increasing temperature, indicating that the activated complex was not stable and the probability of its formation was decreased with increasing of temperature [40].

3.8. Antimicrobial Activity

The inhibition zones were examined for the prepared polymers in the absence and presence of the nanomaterials (ZnOn and Graphene) on two types of bacteria (*S. aureus and E. coli*) at a concentration of800µg/ml.The solvent used was Di - Methyl Sulfoxide (DMSO). The results are listed in Table-4.

Table 4-Inhibition zone values for the polymer in the presence and absence of the nanomaterial.

coating	*Gram positive (S. aureus)*	*(Gram negative) E. coli*
polymer	10	9
Polymer **+ ZnOn**	14	12
Polymer + graphene	28	31
Amoxicillin	30	30
DMSO	-	-

The results showed a good inhibition ability for the polymer,as compared with Amoxicillin, against both *S. aureus* and *E. coli.* The ability of the polymer to kill the bacteria is the function of the stable interaction complex formed between the cleaved DNA and the drug-bound topoisomerases. The inhibition of topoisomerase function by the polymer and the formed stable complexes with DNA has a negative substantial consequence for the cell, as shown by its ability to deal with DNA- damaging drug [41]. Nanomaterials have an increasingly important role in the pharmaceutical and biomedical applications as an antimicrobial strategy against the appearance of antibiotic-resistant strains and the reemergence of infection diseases [42].Nanomaterials are considered as biocidal effective, possibly owing to a combination of their high surface to volume ratio and small size that enable them to intimate the interactions with microbial membranes [43].

4.Conclusion

The corrosion current density (icorr) and corrosion potential (Ecorr) increased with increasing temperature. The corrosion current density (icorr) decreased after coating the S.S with the polymer film in the absence and presence of the nanomaterial. Tafel plots revealed that corrosion potential (Ecorr) of the S.S coated with the polymer film in the absence and presence of the nanomaterial shifts to a higher position as compared to that of the uncoated S.S, implying that the polymer film acts as an anodic protection. Protection efficiency (PE%) was decreased with increasing temperature for the uncoated and coated S.S in the absence and presence of the nanomaterial. The polymer film-coated S.S modified with graphene had a higher protection efficiency (PE%) than the polymer film-coated S.S modified with ZnO_n. AFM and SEM analysis showed that the protection of S.S occurred due to the formation of a protective film on the metal surface. Beside the resistance to corrosion, the polymer film providesan antimicrobial activity against *S. aureus and E. coli* bacteria, with the polymer film modified with nanomaterials having a strong activity against these bacteria species.

References

1. Ellis, D. and Verink, Jr. **1992**. *Corrosion Economic Calculations ASM Handbook*, ASM international, **13**: 838.
2. Hoar, H.P. **1961** Electrochemical principles of the corrosion and protection of metals, *J. Appl.Chem*, **11**: 121- 130.
3. Guimard, N. K., Gomez, N. and Schmidt, C. E. **2007**.Conducting polymers in biomedical engineering. *Progress in Polymer Science*, **32**(8): 876-921.
4. Pringle, J. M., Ngamna, O., Chen, J., Wallace, G. G., Forsyth, M. and MacFarlane, D. R. **2006**. Conducting polymer nanoparticles synthesized in an ionic liquid by chemical polymerisation. *Synthetic metals*, **156**(14): 979-983.
5. Chiarelli, P. A., Johal, M. S., Casson, J. L., Roberts, J. B., Robinson, J. M. and Wang, H. L. **2001**.Controlled Fabrication of Polyelectrolyte Multilayer Thin Films Using Spin-Assembly. *Advanced Materials*, **13**(15): 1167-1171.
6. Ulman, A. **1991**. *An introduction to ultrathin organic films: from Langmuir-Blodgett to self-assembly*, 127, Academic press New York.
7. Decher, G., Hong, J. and Schmitt, J. **1992**. Buildup of ultrathin multilayer films by a self-assembly process: III. Consecutively alternating adsorption of anionic and cationic polyelectrolytes on charged surfaces. *Thin solid films*, **210**: 831-835.
8. Decher, G.**1997**. Fuzzy nanoassemblies: toward layered polymeric multicomposites. *Science*, **277**(5330): 1232-1237.

9. Bertrand, P., Jonas, A., Laschewsky, A., and Legras, R. **2000**. Ultrathin polymer coatings by complexation of polyelectrolytes at interfaces: suitable materials, structure and properties. *Macromolecular Rapid Communications*, **21**(7): 319-348.
10. Hammond, P. T. **1999**.Recent explorations in electrostatic multilayer thin film assembly. *Current Opinion in Colloid & Interface Science*, **4**(6): 430-442.
11. Hammond, P. T. **2004**. Form and function in multilayer assembly: new applications at the nanoscale. *Advanced Materials*, **16**(15): 1271-1293.
12. Holder, E., Tessler, N., and Rogach, A. L. **2008**. Hybrid nanocomposite materials with organic and inorganic components for opto-electronic devices. *Journal of Materials Chemistry*, 18(10): 1064-1078.
13. Joanny, J. **1999**. Polyelectrolyte adsorption and charge inversion. *The European Physical Journal B-Condensed Matter and Complex Systems*, **9**(1): 117-122.
14. Qin, X., Wang, H., Wang, X., Miao, Z., Chen, L., Zhao, W., Shan, M. and Chen, Q. **2010**. Amperometric biosensors based on gold nanoparticles-decorated multiwalled carbon nanotubes-poly (diallyldimethylammonium chloride) biocomposite for the determination of choline. *Sensors and Actuators B: Chemical*, **147**(2): 593-598.
15. Steitz, R., Jaeger, W., and Klitzing, R. v. **2001**. Influence of charge density and ionic strength on the multilayer formation of strong polyelectrolytes. *Langmuir*, **17**(15): 4471-4474.
16. Dubas, S. T. and Schlenoff, J. B. **2001**. Swelling and smoothing of polyelectrolyte multilayers by salt. *Langmuir*, **17**(25): 7725-7727.
17. Blomberg, E., Poptoshev, E., Claesson, P. M. and Caruso, F. **2004**. Surface interactions during polyelectrolyte multilayer buildup. 1. Interactions and layer structure in dilute electrolyte solutions. *Langmuir*, **20**(13): 5432-5438.
18. Guo, Y., Geng, W. and Sun, J. **2008**. Layer-by-Layer Deposition of Polyelectrolyte−Polyelectrolyte Complexes for Multilayer Film Fabrication. *Langmuir*, **25**(2): 1004-1010.
19. Ladam, G., Schaad, P., Voegel, J., Schaaf, P., Decher, G., and Cuisinier, F. **2000**. In situ determination of the structural properties of initially deposited polyelectrolyte multilayers. *Langmuir*, **16**(3): 1249-1255.
20. Klitzing, R. v. **2006**. Internal structure of polyelectrolyte multilayer assemblies. *Physical Chemistry Chemical Physics*, **8**(43): 5012-5033.
21. Elzbieciak, M., Zapotoczny, S., Nowak, P., Krastev, R., Nowakowska, M. and Warszynski, P. **2009**. Influence of pH on the structure of multilayer films composed of strong and weak polyelectrolytes. *Langmuir*, **25**(5): 3255-3259.
22. Kolasińska, M. and Warszyński, P. **2005**. The effect of nature of polyions and treatment after deposition on wetting characteristics of polyelectrolyte multilayers. *Applied surface science*, **252**(3): 759-765.
23. Kenawy E.R. **2001**. Biologically active polymers. IV. Synthesis and antimicrobial activity of polymers containing 8-hydroxyquinoline moiety, *J. Appl. Polym. Sci.*, **82**(6): 1364-1374.
24. Kenawy E.R, Worley S.D. and Broughton R. **2007**. The Chemistry and applications of antimicrobial polymers: A State-of-the-Art Review, polymers of high molecular weight have been used, *Biomacromolecules*, **8**(5): 1359-1384.
25. Khulood, A.S. Khalil, S.K. and Muna, I.K. **2018**. Preparation of poly (N-imidazolylmaleamic acid) /nanomaterial coating films on stainless steel by electrochemicalpolymerization to study the anticorrosion and antibacterial action . *Journal of Pharmacy and Biological Sciences*, **13**: 30-36.
26. Léonard-Stibbe, E., Lécayon, G., Deniau, G., Viel, P., Defranceschi, M., Legeay, G. and Delhalle J. **1994**.The cationic polymerization of N-vinyl-2-pyrrolidone initiated electrochemically by anodic polarization on a Pt surfac, *J. Polym. Sci.: Part A, Polym. Chem.*, **32**(8): 1551-1555.
27. Younang, E., Léonard-Stibbe, E., Viel, P., Defranceschi, M., Lécayon, G. and Delhalle J. **1992**. Prospective theoretical and experimental study towards electrochemically grafted poly (N-vinyl-2-pyrrolidone) films on metallic surface, *Molec. Engin*. **1**(4): 317-332.
28. Silverstein R.M., Webster, F.X. and Kiemle, D.J. **1963**.*Spectrometric Identification of Organic Compounds*, 7th ed., John Wiley & Sons, Westford, US.
29. Shirner, R., Fuson, R., Cartin, D. and Mrril, T. **1980**. *The systematic identification of organic compound*, 8th ed., John Wiley & Sons, Ne.
30. Koj, N. **1962**.*Infrared absorption spectroscopy*, 1st ed., Nankodo Cmpany Limited, Tokyo.

31. Zheng, J., Liu, L., Ji, G., Yang, Q., Zheng, L. and Zhang, J. **2016**. Hydrogenated Anatase TiO2 as Lithium-Ion Battery Anode: Size–Reactivity Correlation. *ACS applied materials & interfaces*, **8**(31): 20074-20081.
32. Divij V. and R. K. Goyal. **2014**. Thermal and Dielectric Properties of High Performance Polymer/ZnO Nanocomposites. *Materials Science and Engineering*. **64**: 1-10.
33. Valeria, A., Daniele, N., Roberta, S., Sergio, S., Massimo, P., Jos, M., Giulio, M. and Alberto, M. **2011**. In situ production of high filler content graphene-based polymer nanocomposites by reactive processing. *J Mater Chem*. **21**: 16544–16549.
34. Heitz, E. and Schwenk, W. **1976**. Theoretical basis for the determination of corrosion rates from polarization resistance: prepared for the european federation of corrosion working partyon "Physiocochemical testing method of corrosion fundamentals and application", *British Corrosion J*., **11**(2): 74-77.
35. Tretherwey, K.R. and Chamberlain, J. **1996**. *Corrosion for Science and Engineering*, 2nd, ed., Addision Wesley Longman Ltd.
36. Jalal M. and Yousif K. **1989**. Inhibiting Effects of Ethanethiol, Dimethyl Sulfide, and Dimethyl Disulfide on the Corrosion of Stainless Steel (405) in Sulfuric Acid. *Bulletin of the Chemical Society of Japan*, **62**: 1237.
37. Enders, D. and Shilvock, J. P. **2000**. Some recent applications of α- amino nitrile chemistry, *Chemical Society Reviews*, **29**(5): 359-373.
38. Fontana, M. and Greene, N.**1986**.*Corrosion engineering*: New York: McGraw- Hill.
39. Gomma, M. and Wahdan, M.**1995**. Corrosion behavior of Zn in alchol- water solvents. *Mater. Chem. Phys*, **39**(3): 209-213.
40. Abdulkareem, M.A. and Rawaa, A.M. **2014**. An investigation of electropolymerization and corrosion protection properties of polypyrrole coating on carbon steel and stainless steel,M.Sc. Thesis, Department of Chemistry, College of science, University of Baghdad, Baghdad, Iraq.
41. Kohanski M.A., Dwyer DJ., and Collins JJ. **2010**. How Antibiotics Kill Bacteria: from Targets to Networks, Nature Reviews: Microbiology, **8**: 423-435.
42. Abd El-Rehim, S.S. Hassan, H.H. Amin, M.A. **2001**. Corrosion inhibition of aluminium by 1, 1(lauryl amido) propyl ammonium chloride in HCl solution, *Mater.Chem.Phys*., **70**(1): 64-72.
43. Osama, M.M. Omar, A.M. **1997**. Corrosion inhibition of benzyl triethanol chloride and its ethoxylate on steel in sulphuric acid solution, *Mater.Chem.Phys.*, **50**(3): 271-274.